Inorganic Chemistry

Article

pubs.acs.org/IC

Field-Induced Multiple Relaxation Mechanism of $Co^{III}_2Dy^{III}$ Compound with the Dysprosium Ion in a Low-Symmetrical Environment

Shufang Xue,[†] Liviu Ungur,*[,‡] Yun-Nan Guo,[§] Jinkui Tang,*[,†] and Liviu F. Chibotaru[‡]

[†]State Key Laboratory of Rare Earth Resource Utilization, Changchun Institute of Applied Chemistry, Chinese Academy of Sciences, Changchun 130022, P. R. China

[‡]Theory of Nanomaterials Group, Department of Chemistry, Katholieke Universiteit Leuven, Celestijnenlaan 200F, 3001 Leuven, Belgium

[§]School of Science, Xi'an Jiaotong University, Xi'an, 710049, P. R. China

Supporting Information

ABSTRACT: A defective cubane-shaped heterometallic trinuclear $Co^{III}_2Dy^{III}$ compound with only one magnetically interesting ion (Dy^{III}) has been assembled by virtue of a multifunctional acylhydrazone ligand. Because of the nonaxial ground state of Dy^{III} ion derived from a low-symmetrical crystal field, the title compound displays field-induced multiple relaxation processes which are of molecular and a dipolar−dipolar coupling origin, as revealed by combined experimental and theoretical investigations. The results demonstrate that such a mononuclear dysprosium(III) compound with a low-symmetrical environment of magnetic center appears to be a model system for further investigations to shed light on the complex relaxation mechanism of lanthanide-based single ion magnets.

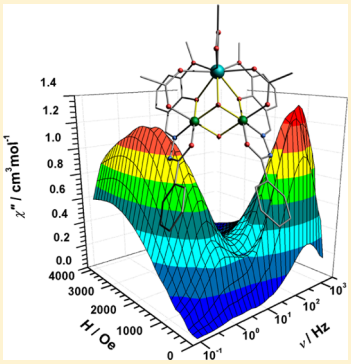

INTRODUCTION

With the driving force of information storage materials and electronic devices to miniaturization, the field of molecular magnets is emerging that combines the advantage of the molecular scale with the properties of bulk magnetic materials and the potential for high-density information storage and quantum computing.[1] In fact, the pioneering work in molecular nanomagnetism dates back to 1993, in which it was shown that dodecanuclear manganese coordination clusters can retain slow relaxation for years below 2 K.[2] This breakthrough started a search for single molecule magnets (SMMs)[3] with "improved" properties referred to as high anisotropy barrier and blocking temperature accessible to practical use. A key condition for achieving the high-performance SMMs is the effective involvement of the anisotropy of the metal sites.[4] In this respect, several important benchmarks are held by mono- and multinuclear lanthanide-based systems by virtue of the large unquenched orbital contribution to the moment and the resulting high magnetic anisotropy.[5]

We have just focused on one branch of SMMs, those containing only one spin carrier. So far Ln-containing mononuclear compounds have been recently developed to a large extent, and suitable strategies have been established in a theoretic and practical sense.[6] The general approach adopted in the design of single ion magnets (SIMs) hinges around the favorable ligand field with high symmetry to dictate the M_J ground state and enhance single-ion anisotropy. This can be explained by the electrostatic model that the Tb^{III} or Dy^{III} ion where the oblate shape of electron density in the ground state needs an axially symmetrical sphere to reserve high anisotropy, while for Er^{III} the equatorially coordinating geometry is preferable so as to minimize charge contact with the axially located f-element electron density.[7] Two representative examples are terbium phthalocyanine compound $(Bu_4N)[Tb(Pc)_2]$[6a,8] and erbium cyclooctatetraene molecule $[Er(COT)_2]^-$,[6g] in which the Tb^{III} ion was in a symmetry close to D_{4d} and the Er^{III} ion preserved a highly D_{8d} symmetry. Those perfect axialities resulted in completely suppressed quantum tunneling of magnetization (QTM) in the ground state and the occurrence of typical SMMs behavior. When the axial symmetry around the metallic center gradually departed from the ideal high symmetry or converted to a low symmetric environment, the transverse tensor of anisotropy induced increased quantum tunneling of magnetization (QTM) in the absence of an external field; in this case, slow relaxation can be observable unless there is application of an optimal field, whose molecules are referred to as field-induced SMMs. Recently the field-induced slow magnetization relaxation and field-tunable multiple relaxation pathways that predominated in several $4f^9$ or $5f^{10}$ systems have yet to be well understood. However, the relaxation mechanism especially the slow relaxation phase

Received: October 6, 2014
Published: November 13, 2014

   dx.doi.org/10.1021/ic502443g | Inorg. Chem. 2014, 53, 12658−12663

corresponding to low frequency domain is still unclear. Inspired by this, we particularly emphasize the origin and conditions necessary for the magnetic moment of individual ions or molecules to be blocked and for their future improvements. Herein, a heterometallic $Co^{III}_2Dy^{III}$ compound synthesized through employing the multifarious acylhydrazone Schiff base ligand H_2hmb (Scheme S1 in Supporting Information, H_2hmb = 2-hydroxy-3-methoxybenzylidene benzohydrazide) displays field-dependent multiple relaxation pathways, originating from the single-ion behavior and intermolecular dipolar interaction as revealed by combined experimental and theoretical investigations.

EXPERIMENTAL SECTION

General Procedures. All chemicals were used as commercially obtained without further purification. Elemental analysis for carbon, hydrogen, and nitrogen were carried out on a PerkinElmer 2400 analyzer. Fourier transform infrared (FTIR) spectra were recorded with a PerkinElmer FTIR spectrophotometer using the reflectance technique (4000−300 cm^{-1}). Samples were prepared as KBr disks. All magnetization data were recorded on a Quantum Design MPMS-XL7 SQUID magnetometer. The variable-temperature magnetization was measured with an external magnetic field of 1000 Oe in the temperature range of 1.9−300 K. Samples were restrained in eicosane to prevent torquing. The experimental magnetic susceptibility data were corrected for the diamagnetism estimated from Pascal's tables[11] and sample holder calibration.

X-ray Crystallography. Crystallographic data were collected on a Bruker Apex II CCD diffractometer with graphite monochromated Mo-Ka radiation (λ = 0.71073 Å). Data processing was accomplished with the SAINT processing program. The structure was solved by direct methods and refined on F^2 by full-matrix least-squares using SHELXTL97.[12] The location of Ln atom was easily determined, and O, N, and C atoms were subsequently determined from the difference Fourier maps. The non-hydrogen atoms were refined anisotropically. The H atoms were introduced in calculated positions and refined with fixed geometry with respect to their carrier atoms. CCDC-1010413 and 1010414 contain the supplementary crystallographic data for this paper. These data can be obtained free of charge from the Cambridge Crystallographic Data Centre via www.ccdc.cam.ac.uk/data_request/cif.

Synthesis of $[Co_2Dy(hmb)_2(CH_3O)_2(OAc)_3]\cdot 2CH_3CN\cdot CH_3OH\cdot H_2O$ (1). To a slurry of H_2hmb (0.2 mmol, 54.2 mg) and triethylamine (0.028 mL, 0.2 mmol) in CH_3OH/CH_3CN (10 mL/10 mL), solid $Dy(OAc)_3\cdot H_2O$ (0.2 mmol, 71.5 mg) was added. After the mixture was stirred for 2 h, $Co(OAc)_2\cdot 4H_2O$ (49.6 mg, 0.2 mmol) was added to the resulting yellow solution. Then the mixture was stirred for another 3 h, followed by filtration. Brown block-shaped single crystals of $[Co_2Dy(hmb)_2(CH_3O)_2(OAc)_3]\cdot 2CH_3CN\cdot CH_3OH\cdot H_2O$ (**1**), suitable for X-ray diffraction analysis formed after 3 days. Yield: 42 mg (35%, based on the Lu^{III}). Anal. Calcd (found) for $C_{43}H_{51}N_6O_{16}Co_2Dy$: C, 43.46 (43.16); H, 4.33 (4.30); N, 7.07 (6.98). IR (KBr, cm^{-1}): 3419 (br), 2936 (w), 2832 (w), 2248 (w), 1608 (w), 1584 (s), 1548 (s), 1506 (s), 1493 (s), 1434 (s), 1384 (s), 1347 (m), 1283 (w), 1243 (s), 1225 (m), 1183 (w), 1170 (w), 1098 (w), 1070 (w), 1019 (w), 963 (w), 922 (w), 862 (w), 776 (w), 731 (s), 705 (w), 684 (m), 619 (w), 592 (w).

Synthesis of $[Co_2Lu(hmb)_2(CH_3O)_2(OAc)_3]\cdot 2CH_3CN\cdot CH_3OH\cdot H_2O$ (2). The preparation of this compound follows the same procedure as for **1** except that $Lu(OAc)_3\cdot H_2O$ (0.2 mmol, 74 mg) was used as the starting material instead of $Dy(OAc)_3\cdot H_2O$. The clear solution was left at room temperature for 3 days to afford brown block crystals $[Co_2Lu(hmb)_2(CH_3O)_2(OAc)_3]\cdot 2CH_3CN\cdot CH_3OH\cdot H_2O$ (**2**). Yield: 39 mg (33%, based on the Dy^{III}). Anal. Calcd (found) for $C_{43}H_{51}N_6O_{16}Co_2Lu$: C, 43.67 (43.36); H, 4.18 (4.09); N, 7.11 (6.98). IR (KBr, cm^{-1}): 3419 (br), 2936 (w), 2832 (w), 2248 (w), 1608 (w), 1584 (s), 1548 (s), 1506 (s), 1493 (s), 1434 (s), 1384 (s), 1347 (m), 1283 (w), 1243 (s), 1225 (m), 1183 (w), 1170 (w), 1098 (w), 1070 (w), 1019 (w), 963 (w), 922 (w), 862 (w), 776 (w), 731 (s), 705 (w), 684 (m), 619 (w), 592 (w).

Synthesis of Dilution Sample $Dy_{0.05}Lu_{0.95}Co_2$. The site substituted samples $Dy_{0.05}Lu_{0.95}Co_2$ was synthesized in accordance with the synthesis of pure **1** (see above), with accurately measured 19:1 molar ratios of the lutetium(III) and dysprosium(III) acetate starting materials.

RESULTS AND DISCUSSION

Compound **1** with the formula $[Dy^{III}Co^{III}_2(hmb)_2(CH_3O)_2(OAc)_3]\cdot 2CH_3CN\cdot CH_3OH\cdot H_2O$ was obtained as dark red crystals from the reaction of $Dy(OAc)_3\cdot H_2O$, $Co(OAc)_2\cdot 4H_2O$ with acylhydrazone Schiff base ligand H_2hmb, which has been reported in the assembly of mononuclear dysprosium compound.[13] Single-crystal X-ray diffraction measurements revealed that compound **1** crystallized in the triclinic space group $P\bar{1}$ (Table 1). The detailed data of the bond lengths and angles are listed in Table S1, Supporting Information. The structure was found to be a heterometallic trinuclear cluster involving two cobalt and one dysprosium elements. Charge balance in combination of the metric parameters and bond-valence-sum calculations (Table S2, Supporting Information) reveals that the cobalt element is attributable to the trivalent oxidation state and diamagnetic character in agreement with the experimentally empirical analysis that the basic conditions facilitate the oxidation of Co^{II} to Co^{III} by atmospheric O_2 gas.[14] A perspective view of the $[Dy^{III}Co^{III}_2O_4]$ metallic core represents a defective cubane, where the metallic centers (Figure 1) are held together primarily via one deprontonated μ_3 methoxide (O13), one deprontonated μ-methoxide (O14), and two μ-hydroxide (O2 and O5) ligands with the Co···Co and Co···Dy separations of 2.907(1), 3.3476(9), and 3.3570(8) Å, respectively. Around the periphery of core are two compartmental ligands that coordinate via the tridente ONO pocket to the Co^{III} ion and the *o*-vanillin to the Dy^{III} ion. Besides, two acetate ions in syn-syn $\eta^1{:}\eta^1{:}\mu_2$ chelate one Co^{III} and one Dy^{III} ion. The Co^{III} ions

Table 1. Crystallographic Data and Structure Refinement for 1 and 2

compound	1	2
formula	$C_{43}H_{51}N_6O_{16}Co_2Dy$	$C_{43}H_{51}N_6O_{16}Co_2Lu$
M_r	1188.26	1200.73
color	brown	brown
crystal system	triclinic	triclinic
space group	$P\bar{1}$	$P\bar{1}$
T [K]	191(2)	298(2)
a [Å]	12.0987(7)	12.1849(7)
b [Å]	14.2213(8)	14.2833(8)
c [Å]	14.2303(8)	14.4822(8)
α [deg]	98.3600(10)	98.9744(11)
β [deg]	105.6000(10)	106.2809(10)
γ [deg]	97.5520(10)	96.8021(12)
V [Å^3]	2295.5(2)	2354.6(2)
Z	2	2
ρ_{calcd} [g cm^{-3}]	1.719	1.694
μ(Mo KR) [mm^{-1}]	2.403	2.853
F(000)	1198	1208
R_{int}	0.0268	0.0238
R_1 [$I > 2\sigma(I)$]	0.0430	0.0354
wR_2 (all data)	0.1253	0.0889
GOF	1.067	1.031

dx.doi.org/10.1021/ic502443g | Inorg. Chem. 2014, 53, 12658−12663

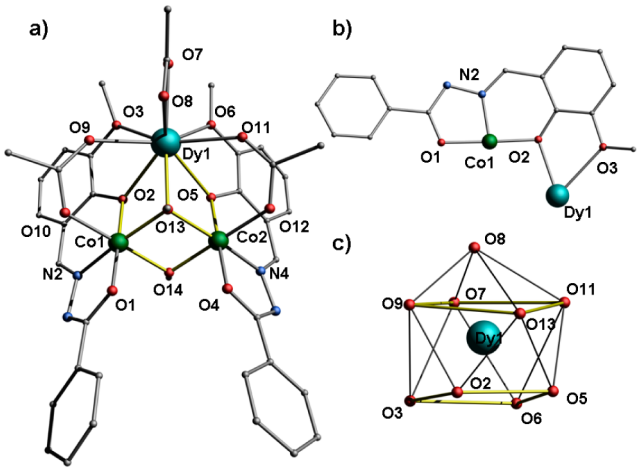

Figure 1. Representation of the structure of $Co^{III}_2Dy^{III}$ entity (a), the coordination mode of ligand (b) as well as the coordination sphere of Dy^{III} centers (c) in **1**.

are coordinated to five oxygen and one nitrogen atoms which give rise to an octahedral geometry that displays an average Co−$L_{N,O}$ bond distance of 1.899(4) Å. For the paramagnetic Dy^{III} ion, there is a terminal acetate ion bounded to the Dy^{III} ion, thus making it nine-coordinate with the intuitionistic view of the geometry being a monocapped distorted square antiprism and an average Dy−O bond length of 2.406(4) Å. Exact geometry analysis by SHAPE 2.0 software[15] (Table S3, Supporting Information) reveals that geometry of the nine-coordinated lanthanide ion and six-coordinated cobalt ions are monocapped square antiprism with the deviation of 1.042 from the ideal C_{4v} symmetry and octahedral geometry, respectively. Further inspection of the supramolecular arrangement reveals that the shortest intermolecular Dy···Dy distance is 8.145 Å (Figure S1, Supporting Information).

Magnetic Properties. Magnetic measurements were performed on polycrystalline samples of **1** using Quantum-Design MPMS magnetometers. It was found that the temperature dependence of its molar magnetic susceptibility is characteristic of noninteracting mononuclear dysprosium(III) compounds. The corresponding $\chi_M T$ vs T plot is provided in Figure S2, Supporting Information. The room-temperature $\chi_M T$ value is 14.46 cm^3 K mol^{-1}, which is in agreement with a single noninteracting $4f^9$ Dy^{III} ion.[16] It remains roughly constant at the high temperature range and then decreases slightly down to 10.06 cm^3 K mol^{-1} at 2 K due to the thermal depopulation of the $^6H_{15/2}$ ground state of the Dy^{III} ion and/or intermolecular magnetic dipole−dipole interaction. The magnetization was measured up to 7 T dc field at 1.9, 3, and 5 K, respectively. The nonsuperposition of the M vs H/T plots at higher field (inset, Figure S2, Supporting Information) implies the presence of significant magnetic anisotropy.

The dynamic magnetic properties of **1** were further probed by using ac measurements under 3 Oe field. The imaginary component of the ac susceptibility is almost negligible under a zero dc field (Figure S3, Supporting Information), but becomes significantly more intense under a small applied dc field as exemplified in Figure 2. Usually in those field-induced SMMs the application of a static field makes a dominant contribution to the effective suppression of underbarrier mechanism, as witnessed in the shift of the maxima in the imaginary component χ'' from the invisible toward the visible state in

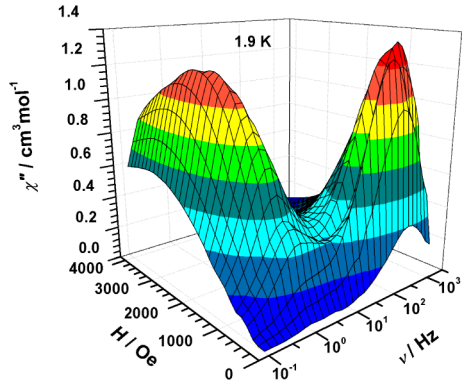

Figure 2. Three-dimensional plots resuming the frequency and field dependence of the imaginary component of the susceptibility of **1** at T = 1.9 K evidencing the presence of two distinct mechanisms of relaxation.

the experimental window.[17] The application of dc field at 1.9 K does indeed dramatically alter the profile of the χ'' frequency scan as shown in a three-dimensional plot (Figure 2). At each field above 500 Oe, the peak observed at 300 Hz with increasing applied field gradually diminishes, while a much lower-frequency peak simultaneously intensifies. This change continues until 2.5 kOe, at which point the intensity of a high-frequency peak is nearly uncompetitive with those of the low-frequency maximum (Figure S4, Supporting Information).

The relaxation times extracted from $\chi''(\nu)$ under different applied static fields (Figure S4, Supporting Information) using the sum of two modified Debye functions[18] are reported in Figure 3 for two processes with distinct field dependence.

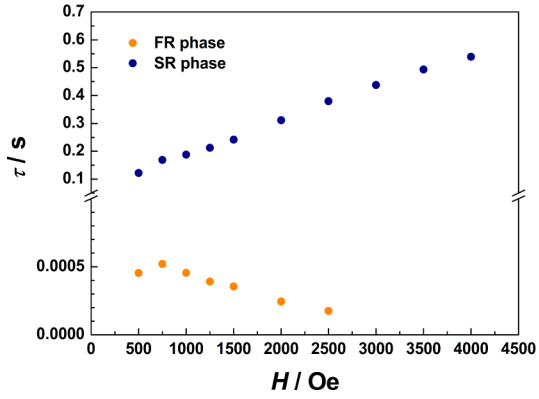

Figure 3. Field dependence of the magnetic relaxation time at 1.9 K for two relaxation processes occurring in the SR and FR phase.

Interestingly, slow relaxation (SR) process presents a field-dependent slowing down with a three-orders slower rate than that of the relaxation pathway operational in the high frequency regime even if in the low field where the fast relaxation is dominant. Increasing the dc field from 500 to 4000 Oe demonstrates an evolution from a fast to slow process within ac frequency window (Figure 4).

To be more informative, the frequency-dependent ac susceptibilities were performed under 500, 1250, and 2500 Oe (Figures 5 and S5). From the 500 Oe data in Figure 5, χ'' becomes strongly frequency-dependent in the whole temperature range with the maximum at higher than 300 Hz. The Arrhenius activation barrier to magnetic relaxation for **1** was determined to be 5.5 K with a large pre-exponential factor of

dx.doi.org/10.1021/ic502443g | Inorg. Chem. 2014, 53, 12658−12663

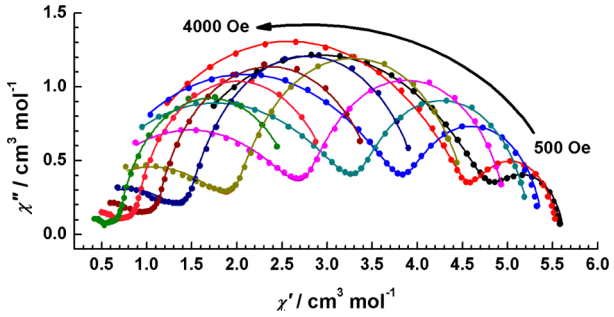

Figure 4. Cole−Cole plots showing the field dependence of multiple relaxation processes occurring in **1** at 1.9 K. Solid lines were performed using the sum of two modified Debye functions.

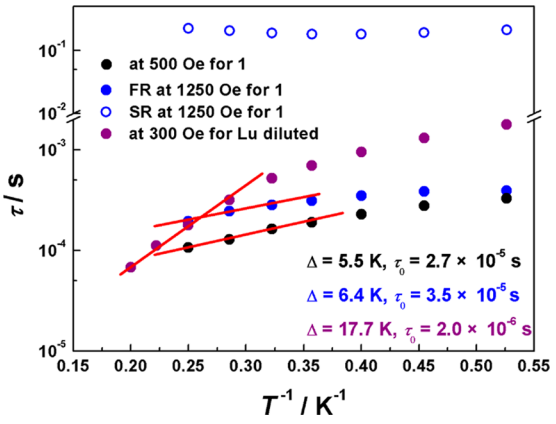

Figure 6. Arrhenius plots of relaxation times of **1** as a pure substance under 500 and 1250 Oe, and diluted in a matrix of Lu^{III} analogue under 300 Oe. The solid line is fitted with the Arrhenius law.

2.7×10^{-5} s. In the case of 1250 and 2500 Oe (Figure 5), two independent relaxation domains were observed at high and low frequency regime, respectively. On the basis of the sum of two modified Debye functions,[18,19] Arrhenius analysis gave an effective energy barrier (Δ) of 6.4 K and a pre-exponential factor (τ_0) of 3.4×10^{-5} s for the FR phase under 1250 Oe. Noteworthy is that the relaxation rate corresponding to the SR phase under 1250 Oe and two relaxation pathways under 2500 Oe eliminate any strong thermal dependence (Figures 6 and S6), suggesting that spin flipping is not involved in a real excited state but a direct process within the ground state Kramers doublet. Given that only one crystallographically independent Dy^{III} ion is present in the system, the field-induced two-step process may be ascribed to single-ion behavior altogether with the dipole−dipole interaction. In essence, the lattice vibrations have been influential in varying the distance between the magnetic ions. As a result, the magnetic field produced by a dipole at a neighboring dipole varies approximately as $(\mu/r^3)/(dr/r)\cos(\omega t)$, where μ is magnetic moment, r is the nearest neighbor distance between dipoles, and dr is the amplitude of the variation of this distance.[20] Therefore, it is the shortest intermolecular Dy···Dy distance equal to 8.145 Å between two nearest neighbors in **1** (Figure S1, Supporting Information) that does not necessarily preclude any intermolecular exchange interactions, and one magnetic ion behaves as an induced dipolar field influencing the relaxation of the other spin center. In contrast to **1**, another recently reported linear $Co^{III}_2Dy^{III}$ compound behaves as a field-induced SMM with an activated barrier of 74.1 K,[14e] where the shortest intermolecular Dy···Dy distance is quite longer (10.408 Å), thus having no practical influence on the magnetic properties. In this regard, we studied the effect of magnetic dilution sample **1a** (5% Dy^{III} doped into a Lu^{III}-based matrix) on the relaxation. Indeed, the ac measurements reveal the significant decrease in the intensity centered at low-frequency domain; therefore, a single dominant relaxation process predominates at 1.9 K when the dc field varies from 300 to 4000 Oe (Figure 7). The

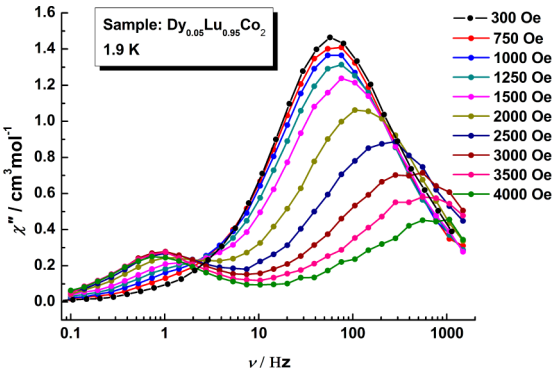

Figure 7. Frequency-dependent imaginary component of ac susceptibility collected on $Dy_{0.05}Lu_{0.95}Co_2$ at 1.9 K under the indicated dc field.

relaxation time at 300 Oe dc field exacted from the frequency dependence of ac susceptibility (Figure 8) follows the Arrhenius law with the energy barrier of 17.7 K and the τ_0 of 2.0×10^{-6} s (Figure 6). The data plotted as Cole−Cole plots (Figure S7, Supporting Information) show a relatively sym-

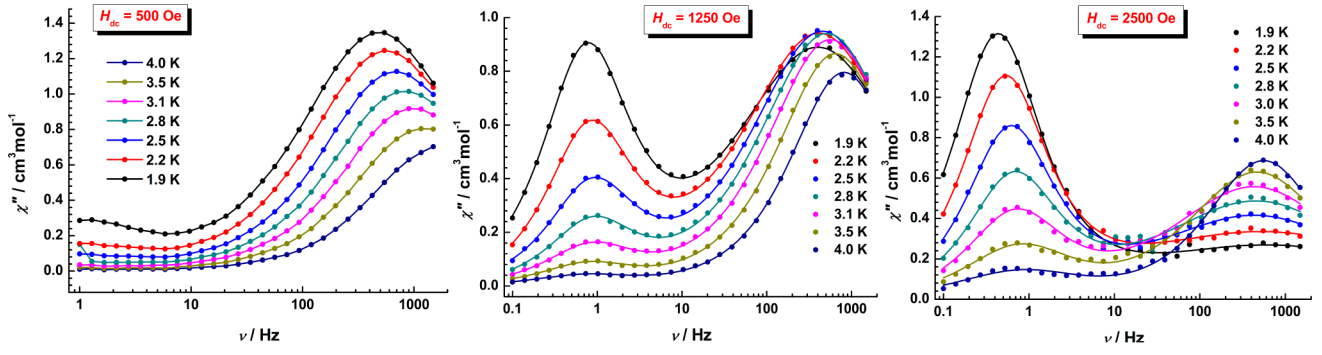

Figure 5. Frequency dependence of the imaginary components of the ac susceptibility of **1** measured at 500, 1250, and 2500 Oe dc field in the temperature range 1.9−4 K. Solid lines were performed using the sum of two modified Debye functions in the case of 1250 and 2500 Oe.

dx.doi.org/10.1021/ic502443g | Inorg. Chem. 2014, 53, 12658−12663

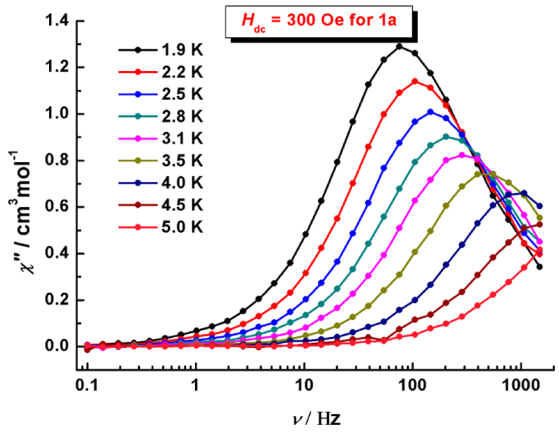

Figure 8. Frequency dependence of the ac susceptibility of **1a** measured at 300 Oe dc field in the temperature range 1.9−5 K.

metrical shape and can be fitted to the generalized Debye model[21] with α parameters below 0.15, indicating that a single relaxation time is mainly involved in the present relaxation process independently of the temperature. Compared with that in the undiluted sample, the relaxation time at 1.9 K is increased by 1 order of magnitude in the diluted sample, in accordance with that found for mononuclear systems.[9c,10b] Furthermore, the energy barrier at 500 Oe and that of the FR at 1250 Oe is significantly increased from 5.5 and 6.4 K in **1** to 17.7 K in **1a**, possibly due to the suppression of QTM derived from the intermolecular dipole−dipole interaction.

Ab initio calculations for compound **1** were performed by using a CASSCF/RASSI-SO approach that includes the spin−orbit coupling[22] and the magnetic properties (Figures S8−S12 and Tables S4 and S5, Supporting Information). Co^{III} is diamagnetic (S = 0 ground state); therefore, the entire paramagnetism comes from the Dy^{III} ion as probably expected. Calculations reveal that the ground Kramers doublet as well as excited doublets are far from being axial. The reason for the absence of magnetic axiality lies in the nature of the crystal field of the ground J = 15/2 of Dy^{III} site. Indeed, as Table S6, Supporting Information shows, the calculated crystal field exerted by the ligand onto the Dy^{3+} magnetic site is far from being axial. All axial parameters (B_2^0, B_4^0, B_6^0) of the crystal field of the ground manifold J = 15/2 are significantly weaker than the nonaxial ones. The main anisotropy axis of the ground doublet of Dy^{III} ion (Figure 9) passes between the O7 and O8, almost bisecting the O7−C−O8 angle.

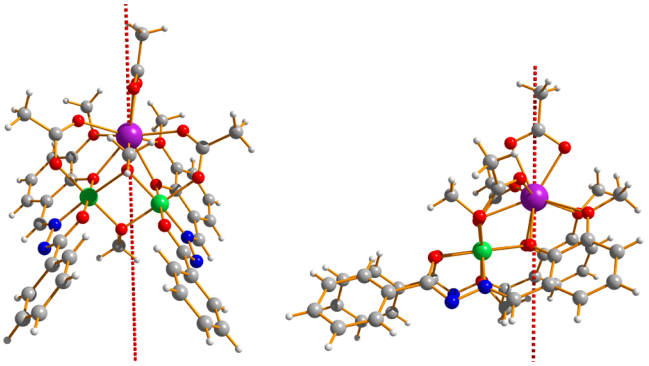

Figure 9. Orientation of the main anisotropy axis of Dy site (g_Z) with respect to molecular frame.

The existence of fast tunneling of magnetization in **1** is supported by the calculated g tensor of the ground Kramers doublet, which is not axial (g_x = 0.6183, g_y = 2.3763, g_z = 17.2113). The non-negligible transverse components g_x and g_y induce the spin flipping via direct process within ground state rather than the Orbach process involved in the excited state as discussed in a nonsandwiched macrocyclic monodysprosium molecule.[17a] On the contrary, those displaying highly efficient SIMs in the absence of external field feature an almost perfectly anisotropy axial ground state due to the presence of high-symmetrical coordination sphere such as D_{4d},[6a,b,d] D_{5h},[9c,23] as well as D_{8h}.[6g] In spite of the nonaxial ground state, for **1**, the magnetic properties of the lowest Kramers doublets still follow the *mirror symmetry* rule; i.e. the axiality of the g tensors gradually decreases up to the Kramers doublets 2 and 3 (Table S5, Supporting Information), and then it starts to increase again reaching for the highest doublet (8), the value being close to M_J = 15/2. The ligand field splitting of the ground $^6H_{15/2}$ atomic multiplet of Dy^{III} is relatively weak (453.7 cm^{-1}), which is a result of relatively long Dy−O bond lengths ($d_{average}$ = 2.406 Å). Additionally, Table S4 shows that the lowest magnetic excitations on Dy^{III} lie at ca. 50 cm^{-1}, which is much higher than the energy barrier obtained from the ac experiment, indicating the real thermal activated regime is out of our ac frequency window, and in current case the relaxation is mainly controlled by quantum tunneling.

It has been already demonstrated that the magnetic dilution[10b] and application of a moderate dc magnetic field[24] play an important role in suppressing ground-state QTM, thus resulting in an increase of the activation barrier. The same principle operates in the title compound: in the pure $Co^{III}_2Dy^{III}$ molecule, QTM is induced from the nonaxial anisotropy of Dy^{III} ion and the intermolecular dipolar interaction between the nearest neighbors ($d_{Dy\cdots Dy}$ = 8.145 Å), SMM behavior emerges upon the optimal applied field; in the doped sample the intermolecular dipolar interactions are reduced, and hence QTM is suppressed to some extent so as to enhance the barrier much closer to the order of magnitude predicted by electronic structure calculations.

CONCLUSION

A heterometallic trinuclear $Co^{III}_2Dy^{III}$ compound has been assembled by virtue of a multifunctional acylhydrazone ligand. Because of the nonaxial ground state of Dy^{III} ion, the title compound displays slow relaxation of magnetization only upon the application of an external dc field and dilution. In particular is that the field-tunable multiple thermally activated relaxation processes are of molecular and dipolar−dipolar coupling origin. The results demonstrate that low-symmetrical coordination sphere and weak dipole couplings between the lanthanide ions especially in mononuclear systems could have a significant impact on speeding up the underbarrier relaxation, thus crippling the possibility of spin-flipping via Orbach process ascending to the real excited state. Such a mononuclear dysprosium(III) compound with a low-symmetrical environment of magnetic center appears to be a model system for further investigations to shed light on the complex magnetism of lanthanide-based SIMs.

dx.doi.org/10.1021/ic502443g | *Inorg. Chem.* 2014, 53, 12658−12663

■ ASSOCIATED CONTENT

Supporting Information

Structure and crystallographic data, plots of magnetic data and ab initio calculations. This material is available free of charge via the Internet at http://pubs.acs.org.

■ AUTHOR INFORMATION

Corresponding Authors

*(J.T.) E-mail: tang@ciac.ac.cn.

*(L.U.) E-mail: liviu.ungur@chem.kuleuven.be.

Notes

The authors declare no competing financial interest.

■ ACKNOWLEDGMENTS

We thank the National Natural Science Foundation of China (Grants 21371166, 21301136 and 21331003) for financial support.

■ REFERENCES

(1) (a) Leuenberger, M. N.; Loss, D. *Nature* **2001**, *410*, 789−793. (b) Timco, G. A.; Carretta, S.; Troiani, F.; Tuna, F.; Pritchard, R. J.; Muryn, C. A.; McInnes, E. J. L.; Ghirri, A.; Candini, A.; Santini, P.; Amoretti, G.; Affronte, M.; Winpenny, R. E. P. *Nat. Nanotechnol.* **2009**, *4*, 173−178.

(2) (a) Sessoli, R.; Gatteschi, D.; Caneschi, A.; Novak, M. A. *Nature* **1993**, *365*, 141−143. (b) Sessoli, R.; Tsai, H. L.; Schake, A. R.; Wang, S.; Vincent, J. B.; Folting, K.; Gatteschi, D.; Christou, G.; Hendrickson, D. N. *J. Am. Chem. Soc.* **1993**, *115*, 1804−1816.

(3) Gatteschi, D.; Sessoli, R.; Villain, J. *Molecular Nanomagnets*; Oxford University Press: Oxford, 2006.

(4) Garanin, D. A.; Jaafar, R. *Phys. Rev. B* **2010**, *81*, 180401.

(5) (a) Zhang, P.; Guo, Y.-N.; Tang, J. *Coord. Chem. Rev.* **2013**, *257*, 1728−1763. (b) Woodruff, D. N.; Winpenny, R. E. P.; Layfield, R. A. *Chem. Rev.* **2013**, *113*, 5110−5148.

(6) (a) Ishikawa, N.; Sugita, M.; Ishikawa, T.; Koshihara, S.-y.; Kaizu, Y. *J. Am. Chem. Soc.* **2003**, *125*, 8694−8695. (b) AlDamen, M. A.; Clemente-Juan, J. M.; Coronado, E.; Martí-Gastaldo, C.; Gaita-Arino, A. *J. Am. Chem. Soc.* **2008**, *130*, 8874−8875. (c) Jiang, S. D.; Wang, B. W.; Su, G.; Wang, Z. M.; Gao, S. *Angew. Chem., Int. Ed.* **2010**, *49*, 7448−7451. (d) Chen, G.-J.; Guo, Y.-N.; Tian, J.-L.; Tang, J.; Gu, W.; Liu, X.; Yan, S.-P.; Cheng, P.; Liao, D.-Z. *Chem.—Eur. J.* **2012**, *18*, 2484−2487. (e) Jiang, S.-D.; Wang, B.-W.; Sun, H.-L.; Wang, Z.-M.; Gao, S. *J. Am. Chem. Soc.* **2011**, *133*, 4730−4733. (f) Meihaus, K. R.; Long, J. R. *J. Am. Chem. Soc.* **2013**, *135*, 17952−17957. (g) Ungur, L.; Le Roy, J. J.; Korobkov, I.; Murugesu, M.; Chibotaru, L. F. *Angew. Chem., Int. Ed.* **2014**, *53*, 4413−4417. (h) Zhang, P.; Zhang, L.; Wang, C.; Xue, S.; Lin, S.-Y.; Tang, J. *J. Am. Chem. Soc.* **2014**, *136*, 4484−4487.

(7) (a) Rinehart, J. D.; Long, J. R. *Chem. Sci.* **2011**, *2*, 2078−2085. (b) Chilton, N. F.; Collison, D.; McInnes, E. J. L.; Winpenny, R. E. P.; Soncini, A. *Nat. Commun.* **2013**, *4*, 2551.

(8) Ishikawa, N.; Sugita, M.; Okubo, T.; Tanaka, N.; Iino, T.; Kaizu, Y. *Inorg. Chem.* **2003**, *42*, 2440−2446.

(9) (a) Car, P.-E.; Perfetti, M.; Mannini, M.; Favre, A.; Caneschi, A.; Sessoli, R. *Chem. Commun.* **2011**, *47*, 3751−3753. (b) Jeletic, M.; Lin, P.-H.; Le Roy, J. J.; Korobkov, I.; Gorelsky, S. I.; Murugesu, M. *J. Am. Chem. Soc.* **2011**, *133*, 19286−19289. (c) Ren, M.; Bao, S.-S.; Ferreira, R. A. S.; Zheng, L.-M.; Carlos, L. D. *Chem. Commun.* **2014**, *50*, 7621−7624.

(10) (a) Rinehart, J. D.; Meihaus, K. R.; Long, J. R. *J. Am. Chem. Soc.* **2010**, *132*, 7572−7573. (b) Meihaus, K. R.; Rinehart, J. D.; Long, J. R. *Inorg. Chem.* **2011**, *50*, 8484−8489.

(11) Boudreaux, E. A.; Mulay, L. N. *Theory and Applications of Molecular Paramagnetism*; John Wiley & Sons,: New York, 1976.

(12) Sheldrick, G. M. *SHELXS-97Program for Crystal Structure Solution*; University of Göttingen: Germany, 1997.

(13) Lin, P.-H.; Korobkov, I.; Burchell, T. J.; Murugesu, M. *Dalton Trans.* **2012**, *41*, 13649−13655.

(14) (a) Zhao, L.; Wu, J.; Xue, S.; Tang, J. *Chem.—Asian J.* **2012**, *2012*, 2419−2423. (b) Langley, S. K.; Chilton, N. F.; Moubaraki, B.; Murray, K. S. *Inorg. Chem.* **2013**, *52*, 7183−7192. (c) Langley, S. K.; Chilton, N. F.; Moubaraki, B.; Murray, K. S. *Chem. Commun.* **2013**, *49*, 6965−6967. (d) Feuersenger, J.; Prodius, D.; Mereacre, V.; Clérac, R.; Anson, C. E.; Powell, A. K. *Polyhedron* **2013**, *66*, 257−263. (e) Liu, C.-M.; Zhang, D.-Q.; Hao, X.; Zhu, D.-B. *Chem.—Asian J.* **2014**, *9*, 1847−1853.

(15) (a) Ruiz-Martínez, A.; Casanova, D.; Alvarez, S. *Chem. -Eur. J.* **2008**, *14*, 1291−1303. (b) Ruiz-Martinez, A.; Casanova, D.; Alvarez, S. *Dalton Trans.* **2008**, *0*, 2583−2591.

(16) Kahn, O. *Molecular Magnetism*; Wiley-VCH: New York, 1993.

(17) (a) Feltham, H. L. C.; Lan, Y.; Klöwer, F.; Ungur, L.; Chibotaru, L. F.; Powell, A. K.; Brooker, S. *Chem. -Eur. J.* **2011**, *17*, 4362−4365. (b) Xue, S.; Zhao, L.; Guo, Y.-N.; Tang, J. *Dalton Trans.* **2012**, *41*, 351−353.

(18) Guo, Y.-N.; Xu, G.-F.; Gamez, P.; Zhao, L.; Lin, S.-Y.; Deng, R.; Tang, J.; Zhang, H.-J. *J. Am. Chem. Soc.* **2010**, *132*, 8538−8539.

(19) Grahl, M.; Kotzler, J.; Sessler, I. *J. Magn. Magn. Mater.* **1990**, *90−1*, 187−188.

(20) Morrish, A. H. *The Physical Principles of Magnetism*; Wiley-IEEE Press: New York, 1965.

(21) (a) Cole, K. S.; Cole, R. H. *J. Chem. Phys.* **1941**, *9*, 341−351. (b) Aubin, S. M. J.; Sun, Z.; Pardi, L.; Krzystek, J.; Folting, K.; Brunel, L.-C.; Rheingold, A. L.; Christou, G.; Hendrickson, D. N. *Inorg. Chem.* **1999**, *38*, 5329−5340.

(22) Karlstrom, G.; Lindh, R.; Malmqvist, P. A.; Roos, B. O.; Ryde, U.; Veryazov, V.; Widmark, P. O.; Cossi, M.; Schimmelpfennig, B.; Neogrady, P.; Seijo, L. *Comput. Mater. Sci.* **2003**, *28*, 222−239.

(23) (a) Liu, J.-L.; Chen, Y.-C.; Zheng, Y.-Z.; Lin, W.-Q.; Ungur, L.; Wernsdorfer, W.; Chibotaru, L. F.; Tong, M.-L. *Chem. Sci.* **2013**, *4*, 3310−3316. (b) Ganivet, C. R.; Ballesteros, B.; de la Torre, G.; Clemente-Juan, J. M.; Coronado, E.; Torres, T. *Chem. -Eur. J.* **2013**, *19*, 1457−1465.

(24) (a) Luzon, J.; Bernot, K.; Hewitt, I. J.; Anson, C. E.; Powell, A. K.; Sessoli, R. *Phys. Rev. Lett.* **2008**, *100*, 247205. (b) Xue, S.; Zhao, L.; Guo, Y.-N.; Chen, X.-H.; Tang, J. *Chem. Commun.* **2012**, *48*, 7031−7033.